

การวิเคราะห์ลักษณะของมะเร็งตับในระยะตับและทางเดินน้ำดีของสาร gadoxetate disodium

จุฬาลักษณ์ พรหมสร¹, มารีนีส พหลภาคย์¹, นิตยา ฉมาดล¹, ปณิตา ลิ้มปะวัฒน์²

¹ภาควิชารังสีวิทยา, ²ภาควิชาอายุรศาสตร์ คณะแพทยศาสตร์ มหาวิทยาลัยขอนแก่น ประเทศไทย

Analysis of Hepatobiliary Phase of Gadoxetate Disodium Characteristics of Hepatocellular Carcinoma

Julaluck Promsorn¹, Mareenis Paholpak¹, Nittaya Chamadol¹, Panita Limpawattana²

¹Department of Radiology, ²Department of Internal Medicine, Faculty of Medicine, Khon Kaen University, Thailand

Received: 28 December 2020/ Edit: 15 February 2021 /Accepted: 6 September 2021

วัตถุประสงค์: เพื่อกำหนดลักษณะของก้อนมะเร็งตับ และศึกษาปัจจัยที่มีความสัมพันธ์กับลักษณะของมะเร็งตับในระยะตับและทางเดินน้ำดีหลังการฉีดสาร gadoxetate disodium

วิธีศึกษา: เป็นการศึกษาย้อนหลังของคนที่ได้รับการตรวจวินิจฉัยโรคด้วยคลื่นแม่เหล็กไฟฟ้า ของผู้ป่วยที่เป็นโรคมะเร็งตับและได้ฉีดสาร gadoxetate disodium ที่โรงพยาบาลศรีนครินทร์ มหาวิทยาลัยขอนแก่น ระหว่างเดือน เมษายน 2552 ถึง ตุลาคม 2554 ข้อมูลประชากร วิเคราะห์โดยใช้สถิติเชิงพรรณนา และใช้การถดถอยโลจิสติกที่ไม่แปรผันเพื่อวิเคราะห์ผลลัพธ์ของการศึกษา

ผลการศึกษา: จากก้อนมะเร็งตับทั้งหมด 45 ก้อน พบลักษณะ hypointensit 39 ก้อน (ร้อยละ 87.2) พบลักษณะ hyperintense 6 ก้อน ซึ่ง 1 ก้อนพบ homogenous hyperintensity และ hypointense บริเวณขอบ และ 5 ก้อนพบ hyperintensity และ hypointense ตรงขอบร่วมกับจุด hypointense ในก้อน ของ ตับและทางเดินน้ำดีหลังการฉีดสาร gadoxetate disodium พบว่าค่า ALT ที่มากกว่า 100 ขึ้นไปสัมพันธ์กับลักษณะก้อนมะเร็งตับที่มีลักษณะ hyperintensity และ hypointense ตรงขอบร่วมกับจุด hypointense ในก้อน ส่วน AFP ขนาดก้อน Child-Pugh ไม่มีความสัมพันธ์กับลักษณะของก้อนมะเร็งตับ ในระยะ ตับและทางเดินน้ำดีหลังการฉีดสาร gadoxetate disodium

สรุป: ก้อนมะเร็งตับส่วนใหญ่ให้ลักษณะ hypointensity และค่า ALT ที่มากกว่า 100 ขึ้นไปสัมพันธ์กับลักษณะก้อนมะเร็งตับที่มีลักษณะ hyperintensity และ hypointense ตรงขอบร่วมกับจุด hypointense ในก้อนในระยะตับและทางเดินน้ำดีหลังการฉีดสาร gadoxetate disodium

คำสำคัญ: มะเร็งตับ; คลื่นแม่เหล็กไฟฟ้า; การทำงานของตับ; ทางเดินน้ำดี; เอนไซม์ของตับ

Objective: To characterize the patterns of hepatocellular carcinoma (HCC) nodules and to determine the factors correlated with the hepatobiliary phase characteristics of the HCC nodules using gadoxetate disodium-enhanced hepatobiliary phase MRI.

Methods: A retrospective review of medical records and dynamic imaging using gadoxetate disodium-enhance MRI of patients with HCC at Srinagarind Hospital, Khon Kaen University, Thailand between April 2011 and October 2013 was performed. Demographic data were analyzed using descriptive statistics. Univariate logistic regressions were used to analyze the outcomes.

Results: Forty-five HCC were eligible for this study; the majority of the HCC patients (39 cases; 87.2%) had hypointensity of HCC nodules in the hepatobiliary phase. Of the 6 patients with hyperintense HCC nodules, 1 showed homogenous hyperintensity with hypointense rims and 5 showed hyperintensity with hypointense rims and focal defects in the hepatobiliary phase. Only ALT ≥ 100 U/L was significantly associated with homogeneous hyperintensity and hyperintense rims with focal defects ($p=0.008$). There was no association between AFP level, size of the HCC nodules, and the Child-Pugh classification with the pattern in the hepatobiliary phase.

Conclusion: In the gadoxetate disodium-enhanced hepatobiliary phase MRI images, the hypointense

*Corresponding author : Dr Julaluck Promsorn, Department of Radiology, Faculty of Medicine, Khon Kaen University, Khon Kaen, 40002, THAILAND, Email:pjulaluck@kku.ac.th

pattern was the most commonly seen in HCC nodules with typical vascular patterns. For HCC appearing as a hyperintense nodule in the hepatobiliary phase, a hypointense rim with a focal defect pattern could be observed. The patients with HCC and ALT ≥ 100 U/L were associated with the hyperintense pattern of the hepatobiliary phase using gadoxetate disodium.

Keywords: Gadoxetate disodium; Hepatocellular carcinoma (HCC); Magnetic resonance imaging (MRI); Child-Pugh; Alanine aminotransferase (ALT); Aspartate aminotransferase (AST); Alpha-fetoprotein (AFP)

ศรีนครินทร์เวชสาร 2564; 36(5):541-549. • Srinagarind Med J 2021; 36(5): 541-549.

Introduction

Hepatocellular carcinoma (HCC) is one of the most common cancers globally and it is associated with high mortality¹. Tumor staging in HCC is crucial in clinical practice since it determines therapeutic choices and establishes prognosis². Various imaging modalities have been proposed for early detection of HCC. The latest guidelines from the American Association for the Study of Liver Diseases (AASLD updated in 2010) indicate that, a diagnosis of HCC can be made by using either biopsies or dynamic imaging (4-phase MDCT or dynamic contrast Magnetic Resonance Imaging (MRI))^{2,3}. A nodule >1 cm with a typical vascular pattern (hypervascular in the arterial phase with washout in the portovenous or delayed phase) can be diagnosed and treated as HCC. If in the first imaging study the nodule did not show a typical vascular pattern, a second contrast-enhanced study with other imaging modalities should be performed. If the nodule still does not demonstrate a typical vascular pattern in any of the studies, a biopsy should be performed to establish a diagnosis^{2,3}.

A recently introduced imaging tool—the liver-specific contrast agent gadoxetate disodium (Primovist®/Bayer) has been used to detect HCC. Immediately after injection the contrast agent has properties of an extracellular matrix agent that provides dynamic perfusion imaging; later, it has the property of a hepatocyte-specific agent that can evaluate delayed hepatocyte uptake and excretion. Gadoxetate disodium enhanced MRI (Gad-EOB-DTPA MRI) reportedly has a high accuracy for detection of HCC^{4,6}. HCCs were usually hypointense against the liver background in the hepatobiliary phase while isointensity or hyperintensity were found 6% and 15% in existing studies^{4,6}. Currently, only a few studies

have been conducted to illustrate the specific hepatobiliary pattern of gadoxetate disodium MRI in HCC. Thus, the primary objective of this study was to characterize the patterns of HCC nodules, and the secondary objective was to determine the factors correlated with the hepatobiliary phase characteristics of HCC nodules, both objectives using gadoxetate disodium.

Materials and Methods

Study design

This was a retrospective study. Study approval was provided by the Ethics Committee for Human Research of Khon Kaen University as instituted by the Helsinki Declaration.

Patient Population and setting

Retrospective medical records and dynamic imaging studies of all patients with HCC who underwent gadoxetate disodium-enhanced MRI at Srinagarind Hospital, Khon Kaen University, Thailand between April 2011 and October 2013 were reviewed. The diagnosis of HCC was based on either pathological proof or the typical vascular pattern in dynamic imaging studies according to the 2010 AASLD Criteria when at least one nodule >1 cm is found, with hypervascularity in the arterial phase and wash out in the portovenous or delayed phases.

Imaging technique

The magnetic resonance imaging (MRI) was performed using 3-T MRI system (Achieva 3.0T TX, Philips Healthcare, Netherlands). All images were obtained with the SENSE-XL-Torso coil. Routine MRI abdomen were acquired with the following sequence:

2D dual-echo breath hold T1W spoiled gradient-echo (GRE) images at opposed phase (TR/effective TE, 134.75/1.15) and inphase (134.75/2.3) with a flip angle of 55, one signal acquired, matrix of 308x224, 6-mm slice thickness, 1 mm gap; triggered T2W single-shot turbo spin-echo images with TR range/ TE, 1015.24/70, echo train length of 76, one signal acquired, matrix of 340x246, 6-mm slice thickness, fat suppression-SPAIR, 1-mm gap; and heavily T2W images with a TR range/TE, 1304.11/180, matrix of 340x244, 4 mm slice thickness, 1-00 gap. For the dynamic MRI, gadoxetic acid disodium (0.025 mmol/kg, Primovist, Bayer Schering Pharma) was administered at 2 mL/s with a power injector (Mallinckrodt, Liebel-Flarsheim, OptistarTM LE) with a rapid bolus 20-mL saline flush. A 3D spoiled GRE sequence with chemical-selective fat suppression was performed before IV injection of the contrast agent. Hepatic arterial phase images were obtained 5 sec after arrival of the contrast medium in the distal thoracic aorta, and portovenous and equilibrium phase images 75 sec and 5 min after beginning the injection. Finally, hepatobiliary phase imaging was obtained 30 min after the beginning of contrast-medium injection. The MRI parameters included TR/TE, 3.05/1.43; flip angle, 10; matrix size 212x169; one signal acquired; a 2-mm slice thickness with interpolation technique.

Data collection

Demographic data and imaging variables were retrospectively collected. Demographic data included age, gender, presence of cirrhosis, hepatitis profiles, liver function tests (AST and ALT), serum AFP, and Child-Pugh classification. For the imaging variables, signal intensities on T1W, T2W, arterial phase, portovenous phase, equilibrium phase and hepatobiliary phase with number, size, location, and other characteristics of nodules were collected. For this analysis a hypointense rim required a thickness of at least 2 mm that encircled at least two-thirds of the circumference at the periphery of the hyperintense nodule. A focal defect pattern was recorded when there was an area of geographic hypointensity less than one-third within a hyperintense nodule, in the hepatobiliary phase. Disagreement regarding the characteristics of the HCC nodules was resolved by consensus at a second session.

Procedure

There are 135 patients with 210 liver nodules who underwent gadoxetate disodium-enhanced MRI at Srinagarind Hospital, Khon Kaen University during the studied period. Patients with nodules without typical dynamic imaging of HCC were excluded. If there were multiple nodules with typical dynamics imaging of HCC in a single patient, only the largest lesion were included. Finally, there were 45 patients eligible for this study as shown in Figure 1. In this group, 6 patients were confirmed as having HCC by pathological proof after liver transplantation and 12 patients were confirmed by intense Lipiodol uptake after transarterial chemoembolization (TACE).

Imaging analysis

From all MRI sequences, the hepatobiliary phase images were independently read by two gastrointestinal radiologists (33 and 9 years' experience in abdominal MRI), who were blinded to the clinical information, final diagnosis, pathological diagnosis and the original radiological report. The readers were informed about the locations of lesions by series and image number with arrows on the images from the picture archiving and communication system (PACS). Each reader separately evaluated signal intensities of the lesions in each sequence as compared to surrounding liver parenchyma, and the signal intensities were then categorized as hypo-, iso- or hyperintense. If any lesion was partially hypointense or hyperintense, it would be categorized based on the dominant signal intensity. Arterial enhancement (defined as higher lesion intensity on the arterial phase than on pre-contrast T1W), washout (defined as hypointensity of the lesion compared with the surrounding liver parenchyma on late phase dynamic images, —portovenous or equilibrium phase) were also recorded.

Statistical analyses

Descriptive data were analyzed using descriptive statistics. Normality of the data was tested using the Shapiro-Wilk test. The variables associated with hypointensity in the hepatobiliary phase of HCC nodules using Gad-EOB-MRI were evaluated using univariate logistic regressions. Odds ratios (OR) and their 95% confidence intervals (CI) were reported to consider the strength of association. Rating agreement between the two readers was analyzed using Kappa statistics. All of the data analyses were performed

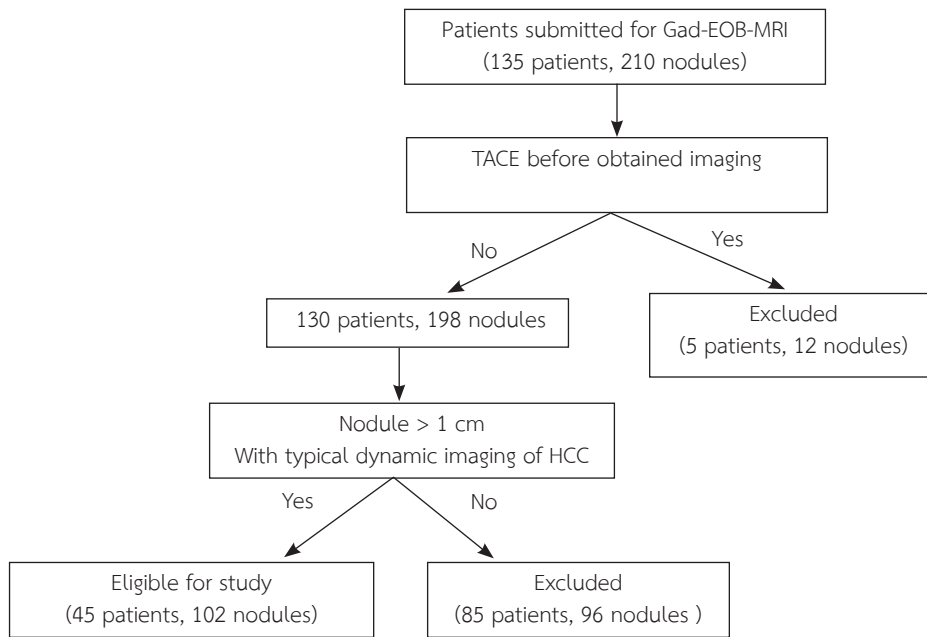


Figure 1 Patients enrollment flow

using SPSS 20 with the level of statistical significance at $p < 0.05$.

Results

Baseline data and MRI characteristic pattern of HCC nodules using Gad-EOB-MRI

Forty-five patients were eligible to review for this study. Demographic and clinical data of them are demonstrated in Table 1. The majority of the nodules were located in the right hepatic lobe and most patients had 1 nodule (55.6%), followed by 2 nodules (20%). Rating agreement between the two readers was 97.1% for intensities in the T1W, T2W, arterial, portovenous, equilibrium and hepatobiliary phases for all of 99 HCC nodules. Three of the HCC nodules were resolved by consensus at a second session. The MRI characteristics of hepatobiliary phase patterns for HCC nodules using gadoxetate disodium-enhanced MRI images are presented in Table 2. The majority of HCC nodules presented as hypointense in the hepatobiliary phase (87.2%) (Figure 2). Of the 6 patients with hyperintense nodules, 5 patients with hypointense rims with focal defects (Figure 3) and 1 patient had homogeneous hyperintensity with hypointense rims (Figure 4).

Clinical data and hepatobiliary characteristics of HCC nodules using Gad-EOB-MRI

Analysis for different patterns found in the hepatobiliary phase of HCC nodules using Gad-

EOB-MRI and clinical data is shown in Table 3. Only ALT > 100 U/L was significantly associated with homogeneous hyperintensity and hyperintense rims with or without focal defects in the hepatobiliary phase. There was no association between AFP level,

ตารางที่ 1 ข้อมูลพื้นฐาน

Parameters	N= 45
Age; years (median, IQR 1,3)	52 (50,56)
Men; n (%)	41 (91.1)
Presence of cirrhosis; n (%)	42 (93.3)
Hepatitis status; n (%)	
No hepatitis	0 (0)
Hepatitis A	1 (2.2)
Hepatitis B	16 (35.6)
Hepatitis C	22 (48.9)
Alcoholic hepatitis	6 (13.3)
Child-Pugh classification; n (%)	
A	36 (80)
B	8 (17.8)
C	1 (2.2)
AFP; ng/ml (median, IQR1,3)	25 (10, 62)
ALT; U/L (median, IQR1,3)	58 (38, 84)
AST; U/L (median, IQR1,3)	66 (48, 111)
Diameter of HCC nodule; cm (median, IQR1,3)	2 (1.3, 2.7)

size of the HCC nodule, Child-Puge classification with the pattern in the hepatobiliary pha

ตารางที่ 2 MRI characteristic patterns of HCC nodules using Gad-EOB-MRI

Parameters	N= 45
T1W finding; n (%)	
Hyperintensity	14 (31.1)
Isointensity	8 (17.8)
Hypointensity	23 (51.1)
T2W finding	
Hyperintensity	45 (100)
Isointensity	0 (0)
Hypointensity	0 (0)
Dynamic phase	
Arterial phase enhancement; n (%)	45 (100)
Porto-venous phase hypointensity; n (%)	45 (100)
Equilibrium phase hypointensity; n (%)	45 (100)
Hepatobiliary phase	
Homogeneous hyperintense with hypointense rim	1 (2.2)
Hyperintense with hypointense rim and focal defect	5 (11.1)
Hypointense	39 (86.7)

Note: HCC; hepatocellular carcinoma

Discussion

This study showed that 86.7% of HCC exhibited hypointensity in the hepatobiliary phase using gadoxetate disodium which is similar to several previous studies. HCC usually demonstrates decreased hepatobiliary uptake in the hepatobiliary phase of gadoxetate disodium. Rhee et al. showed that most early HCCs (93.1%) had decreased hepatobiliary uptake in the hepatobiliary phase using gadoxetate disodium⁴. Three studies⁹⁻¹¹ reported that < 5% of HCC nodules were imaged as hyperintense nodules in the hepatobiliary phase⁷⁻⁹. The other studies reported that between 6 and 15% of hypervascular HCC nodules presented as iso- or hyperintense in the hepatobiliary phase. The finding from the current study is consistent with the previous literature¹⁰⁻¹². There were 13.3 % of cases showing hyperintensity in the hepatobiliary phase of gadoxetate disodium and most of patients showing hyperintense nodules and hypointense rims with focal defects. A focal defect in contrast uptake and the presence of a hypointense rim were the two most important independent MRI findings useful for differentiating hyperintense HCC from benign focal lesions on gadoxetate disodium enhanced hepatobiliary phase images^{13,14}. Previous studies have suggested possible mechanisms for increased uptake of gadoxetate disodium in HCC in hepatobiliary phase images that maybe due to well or moderately differentiated nodules^{11,15,16} and the bile-producing or bile-containing capability of HCC is suggested to be a characteristic

ตารางที่ 3 Comparison of clinical data and characteristic MRI patterns of HCC nodules using Gad-EOB-MRI in hepatobiliary phase

Parameters	Hepatobiliary phase		OR (95%CI)	P-value
	Hyperintensity and hypointense rim ± focal defect N=6 (13.3%)	Hypointensity N=39 (86.7%)		
AFP≥200 ng/ml	1 (14.29)	6 (85.71)	0.9 (0.1,9.2)	0.94
Size ≥1.5 cm	3 (10)	27 (90)	2.3 (0.4,12.8)	0.4
Child-Puge classification				
A	4 (11.1)	32 (88.9)	1	-
B	2 (25)	6 (75)	0.4 (0.1,2.5)	0.3
C	0 (0)	1 (100)	-	-
ALT 100 U/L	4 (66.7)	5 (12.8)	0.1 (0.01, 0.5)	0.008*
AST100 U/L	4 (66.7)	10 (25.6)	0.2 (0.02, 1.1)	0.06

Note: OR; odd ratios, CI; confidence interval, p-value was significant at p<0.05, AFP; alpha fetoprotein, ALT; alanine transaminase, AST; aspartate transaminase, HCC; hepatocellular carcinoma

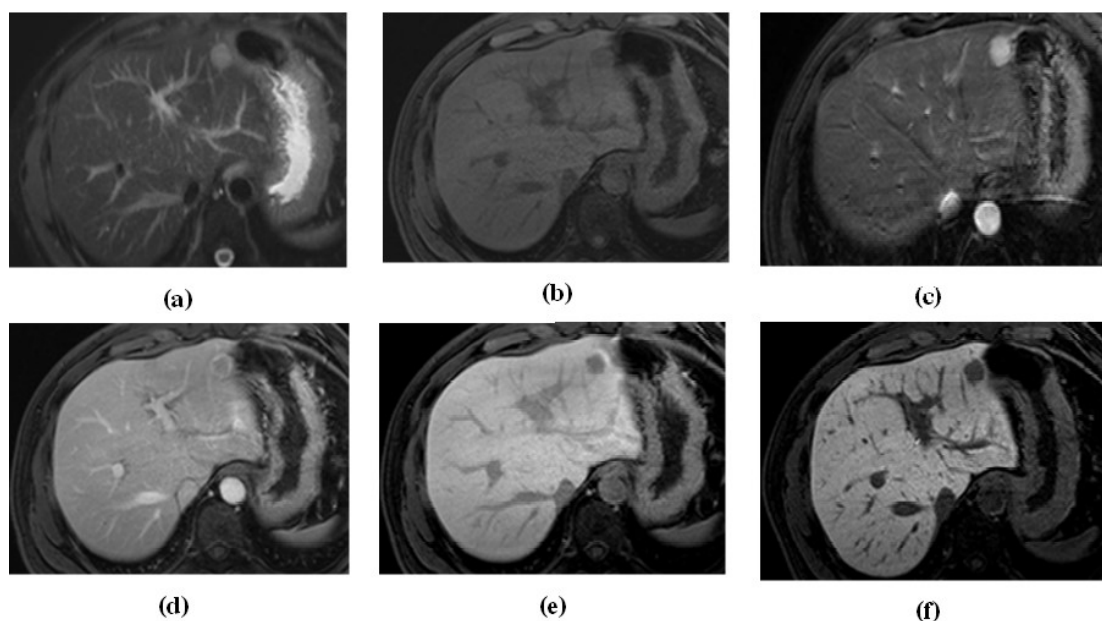


Figure 2 A 51-year-old man with a history of HBV infection with a 2 cm HCC in segment 2 of the liver. Pathological proof found after liver transplantation.

- (a) T2-weighted: the lesion showed hyperintensity.
- (b) Pre-contrast T1-weighted: the lesion showed hypointensity.
- (c) Arterial phase: the lesion showed arterial enhancement.
- (d) Portovenous phase, (e) Equilibrium phase: the lesion showed washout.
- (f) Hepatobiliary phase: the nodule appeared hypointense (no uptake of contrast agent) compared with the surrounding hyperintense liver.

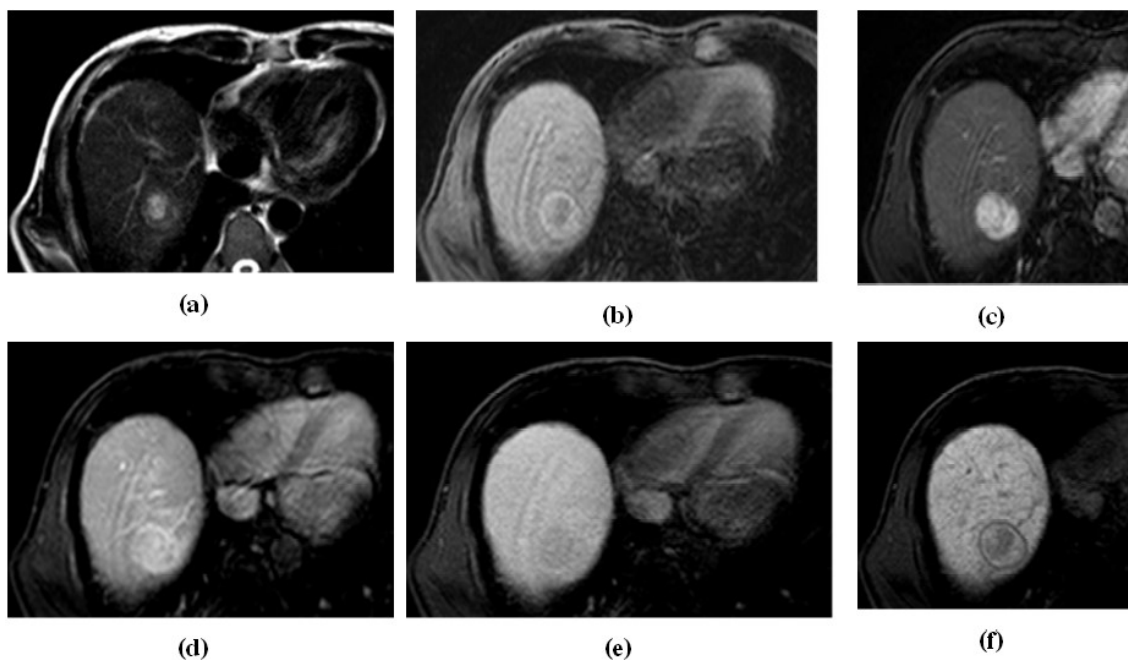


Figure 3 A 55-year-old man with a history of Hepatitis C virus (HCV) infection with a 4.5 cm HCC at segment 8 of the liver and then confirmed having intense Lipodol uptakes after transarterial chemoembolization (TACE).

- (a) T2-weighted: the lesion showed hyperintensity and hypointense rim.
- (b) Pre-contrast T1-weighted: the lesion showed as isointense with a hypointense rim.
- (c) Arterial phase: the lesion showed arterial enhancement.
- (d) Portovenous phase, (e) Equilibrium phase: the lesion showed washout with delayed enhancement of the capsule.
- (f) Hepatobiliary phase: the nodule appeared hyperintense with a focal defect and a hypointense rim compared with the surrounding hyperintense liver.

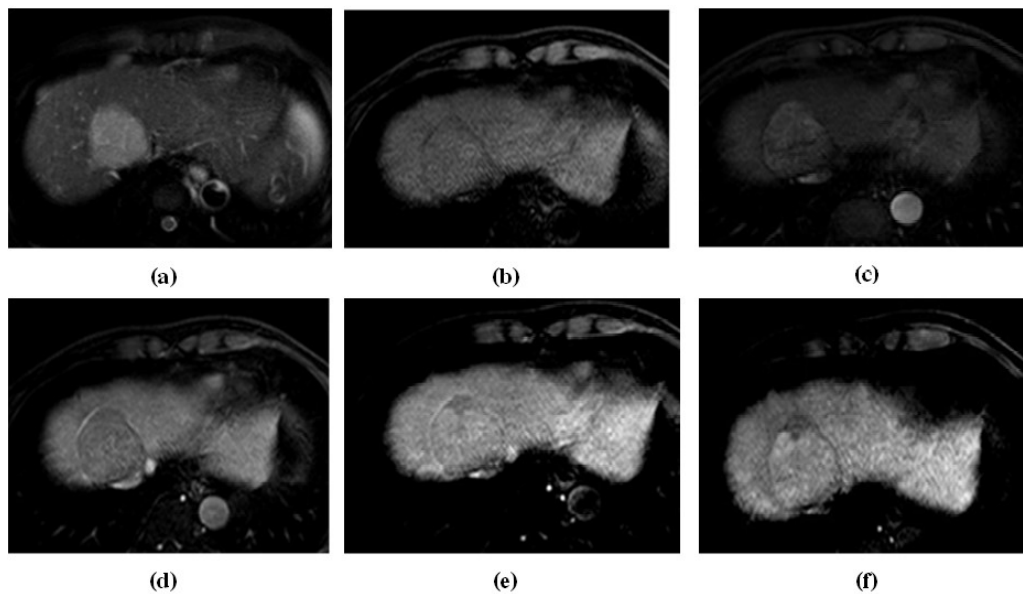


Figure 4 A 53-year-old man with a history of liver HCV cirrhosis with a 1.7 cm HCC in segment 8 of the liver.

(a) T2-weighted: the lesion showed a hyperintensity.

(b) Pre-contrast T1-weighted: the lesion showed as hyperintense.

(c) Arterial phase: the lesion showed arterial enhancement.

(d) Portovenous phase, (e) Equilibrium phase: the lesion showed homogeneous enhancement. (f) Hepatobiliary phase: the nodule appeared hyperintense with a hypointense rim compared with the surrounding liver parenchyma.

of the lesion¹⁷. Malignant liver lesions, especially HCC typically inhibit organic anion-transporting polypeptide 8 (OATP8); therefore, HCC nodules should appear as hypointense lesions in the hepatobiliary phase^{13,14}. This finding could be explained by an intense retention, secondary to over-expression of OATP8 and under expression of multidrug-resistance protein 3 (MRP3) in hyperintense nodule in the hepatobiliary phase using gadoxetate disodium-enhanced MRI^{7-10,14}.

A hypointense rim represented the tumoral fibrous capsule of the HCC nodule¹⁵. A fibrous or pseudocapsule formation is a characteristic finding of HCC and can consist of one of two layers: (a) an inner layer of fibrous material and (b) an outer layer containing compressed vessels and bile ducts¹³. On MRI obtained with extracellular contrast material, a fibrous capsule or pseudocapsule usually has a hypointense rim on both the T1- and T2W images and a hyperintense rim in the equilibrium phase images. This is because of the prominent extracellular matrix in the capsule. Capsules presenting a hypointense rim in the hepatobiliary phase images may be due to the lack of hepatocytes and minimal extracellular enhancement¹³.

This study demonstrated that ALT ≥ 100 U/L was significantly associated with hyperintensity of HCC nodules in the hepatobiliary phase of gadoxetate

disodium. Hepatic parenchymal enhancement in the hepatobiliary phase is mainly determined by liver function in gadoxetate disodium presence which is a decreased uptake in a patient who has poor liver function¹⁸. Hence, in a patient who has poor liver function and a HCC nodule that has an overexpression of OATP8 and underexpression of MRP3, the parenchymal uptake of gadoxetate disodium of the patient with poor liver function should be reduced with an increased uptake in an overexpression of OATP8, and underexpression of a MRP3 HCC nodule causing hyperintensity of the nodule in the hepatobiliary phase of gadoxetate disodium MRI compared to liver parenchyma^{7-10,14,18}.

Kitao et al. reported that a hyperintense HCC had significantly lower expression of AFP than did hypointense HCC¹⁴. This finding; however, did not show the association between the intensity in the hepatobiliary phase of gadoxetate disodium and the other clinical data (AFP level, Child-Pugh classification and tumor sizes). Although, these negative findings might be from lack of a controlled group and the small sample size of the hyperintense group in this study.

There were some limitations of this study. Firstly, the data were collected retrospectively, and therefore some information was lacking. Secondly, the gold standard of HCC diagnosis is the pathological proof

and some patients did not have a tissue biopsy; however; the using typical vascular patterns on dynamic imaging has been accepted in many studies. Thirdly, the sample size of this study is quite low as this technique is limited in some patients due to the high cost of the test. Lastly, we found that HCC with ALT ≥ 100 U/L was associated with a hyperintense pattern in the hepatobiliary phase using Gad-EOB-MRI without further analysis using the multivariate logistic analysis because of the small sample size; therefore, this result could not apply for the general population without underlying hepatitis C cirrhosis. Further study with a greater sample size would be worthwhile.

Conclusions

The results of this study support the previous findings that a pattern of hypointensity in the hepatobiliary phase using Gad-EOB-MRI was the most common pattern seen for HCC nodules with the typical vascular pattern. When HCC nodules display hyperintensity in the hepatobiliary phase, the radiologist should look for specific patterns, such as a hypointense rim with or without focal defect. The patient with HCC and ALT >100 U/L was associated with a hyperintense pattern in the hepatobiliary phase using Gad-EOB-MRI.

Acknowledgements

We wish to acknowledge Professor James A. Will, University of Wisconsin-Madison, for editing the manuscript via the Faculty of Medicine Publication Clinic, Khon Kaen University, Thailand.

Conflicts of interest

None declared.

References

1. El-Serag HB. Hepatocellular carcinoma. *N Engl J Med* 2011; 365: 1118-1127.
2. Bruix J, Sherman M. Management of hepatocellular carcinoma: an update. *Hepatology* 2011; 53: 1020-1022.
3. Leoni S, Piscaglia F, Golfieri R, Camaggi V, Vidili G, Pini P, et al. The impact of vascular and nonvascular findings on the noninvasive diagnosis of small hepatocellular carcinoma based on the EASL and AASLD criteria. *Am J Gastroenterol* 2010; 105: 599-609.
4. Rhee H, Kim MJ, Park MS, Kim KA. Differentiation of early hepatocellular carcinoma from benign hepatocellular nodules on gadoxetic acid-enhanced MRI. *Br J Radiol* 2012; 85: e837-844.
5. Ichikawa T, Saito K, Yoshioka N, Tanimoto A, Gokan T, Takehara Y, et al. Detection and characterization of focal liver lesions: a Japanese phase III, multicenter comparison between gadoxetic acid disodium-enhanced magnetic resonance imaging and contrast-enhanced computed tomography predominantly in patients with hepatocellular carcinoma and chronic liver disease. *Invest Radiol* 2010; 45: 133-141.
6. Ahn SS, Kim MJ, Lim JS, Hong HS, Chung YE, Choi JY. Added value of gadoxetic acid-enhanced hepatobiliary phase MR imaging in the diagnosis of hepatocellular carcinoma. *Radiology* 2010; 255: 459-466.
7. Kogita S, Imai Y, Okada M, Kim T, Onishi H, Takamura M, et al. Gd-EOB-DTPA-enhanced magnetic resonance images of hepatocellular carcinoma: correlation with histological grading and portal blood flow. *Eur Radiol* 2010; 20: 2405-2413.
8. Kim JI, Lee JM, Choi JY, Kim YK, Kim SH, Lee JY, et al. The value of gadobenate dimeglumine-enhanced delayed phase MR imaging for characterization of hepatocellular nodules in the cirrhotic liver. *Invest Radiol* 2008; 43: 202-210.
9. Hamm B, Staks T, Muhler A, Bollow M, Taupitz M, Frenzel T, et al. Phase I clinical evaluation of Gd-EOB-DTPA as a hepatobiliary MR contrast agent: safety, pharmacokinetics, and MR imaging. *Radiology* 1995; 195: 785-792.
10. Narita M, Hatano E, Arizono S, Miyagawa-Hayashino A, Isoda H, Kitamura K, et al. Expression of OATP1B3 determines uptake of Gd-EOB-DTPA in hepatocellular carcinoma. *J Gastroenterol* 2009; 44: 793-798.
11. Kim SH, Lee J, Kim MJ, Jeon YH, Park Y, Choi D, et al. Gadoxetic acid-enhanced MRI versus triple-phase MDCT for the preoperative detection of hepatocellular carcinoma. *AJR Am J Roentgenol* 2009; 192: 1675-1681.
12. Asayama Y, Tajima T, Nishie A, Ishigami K, Kakihara D, Nakayama T, et al. Uptake of Gd-EOB-DTPA by hepatocellular carcinoma: radiologic-pathologic correlation with special reference to bile production. *Eur J Radiol* 2011; 80: e243-248.
13. Suh YJ, Kim MJ, Choi JY, Park YN, Park MS, Kim KW. Differentiation of hepatic hyperintense lesions seen on gadoxetic acid-enhanced hepatobiliary phase MRI. *AJR Am J Roentgenol* 2011; 197: W44-52.
14. Kitao A, Zen Y, Matsui O, Gabata T, Kobayashi S, Koda W, et al. Hepatocellular carcinoma: signal intensity at gadoxetic acid-enhanced MR imaging--correlation with molecular transporters and histopathologic features. *Radiology* 2010; 256: 817-826.

15. Huppertz A, Haraida S, Kraus A, Zech CJ, Scheidler J, Breuer J, et al. Enhancement of focal liver lesions at gadoxetic acid-enhanced MR imaging: correlation with histopathologic findings and spiral CT--initial observations. *Radiology* 2005; 234: 468-478.
16. Fujita M, Yamamoto R, Fritz-Zieroth B, Yamanaka T, Takahashi M, Miyazawa T, et al. Contrast enhancement with Gd-EOB-DTPA in MR imaging of hepatocellular carcinoma in mice: a comparison with superparamagnetic iron oxide. *J Magn Reson Imaging* 1996; 6: 472-477.
17. Shimofusa R, Ueda T, Kishimoto T, Nakajima M, Yoshikawa M, Kondo F, et al. Magnetic resonance imaging of hepatocellular carcinoma: a pictorial review of novel insights into pathophysiological features revealed by magnetic resonance imaging. *J Hepatobiliary Pancreat Sci* 2010; 17: 583-589.
18. Kim JY, Lee SS, Byun JH, Kim SY, Park SH, Shin YM, et al. Biologic factors affecting HCC conspicuity in hepatobiliary phase imaging with liver-specific contrast agents. *AJR Am J Roentgenol* 2013; 201: 322-331.

SMJ